01 Nov 2023

Cement-Based Materials With Solid-Gel Phase Change Materials For Improving Energy Efficiency Of Building Envelope

Zhuo Liu

Jiang Du

Ryan Steere

Joshua P. Schlegel
Missouri University of Science and Technology, schlegelj@mst.edu

et. al. For a complete list of authors, see https://scholarsmine.mst.edu/nuclear_facwork/552

Recommended Citation

Z. Liu et al., "Cement-Based Materials With Solid-Gel Phase Change Materials For Improving Energy Efficiency Of Building Envelope," *Journal of Materials in Civil Engineering*, vol. 35, no. 11, article no. 04023425, American Society of Civil Engineers, Nov 2023.
The definitive version is available at https://doi.org/10.1061/JMCEE7.MTENG-15925

Cement-Based Materials with Solid–Gel Phase Change Materials for Improving Energy Efficiency of Building Envelope

Zhuo Liu, M.ASCE[1]; Jiang Du, M.ASCE[2]; Ryan Steere, M.ASCE[3]; Joshua P. Schlegel, M.ASCE[4]; Kamal H. Khayat, M.ASCE[5]; and Weina Meng, M.ASCE[6]

Abstract: This paper evaluated the cement-based materials incorporated with novel solid–gel phase change materials (PCMs) for improving the energy efficiency of building envelopes. This novel PCM is form-stable, which will not leak as solid–liquid PCMs do and not need encapsulation, and it features high energy-storage capacity. Experimental results showed that the thermal properties of cement-based materials were improved as the increase of PCM content. A 30% replacement of sand by volume with PCM can increase the latent heat of the mixture from around 0 to 7 J/g and decrease the thermal conductivity of PCM mortar based on the generalized self-consistent (GSC) model by about 20%. However, the workability and mechanical properties were compromised. The simulation results indicated that 30% PCM-incorporated walls can contribute to 5% energy saving for cooling in a whole year and 12% reduction in peak cooling load compared with the reference without PCM. The proposed PCM composite offers a promising avenue to achieve energy-efficient building envelopes.
DOI: 10.1061/JMCEE7.MTENG-15925.

Introduction

The energy demand in building structures is expected to rise by about 50% in 2050, and the cooling demand will increase twofold from 2010 to 2050 (Souayfane et al. 2016). The increased energy consumption represents significant capital investment and impacts on the environment. It was estimated that by 2100, climate change will increase the retail cost of electricity by $167 billion in the United States and will lead to $31 billion more in annual purchases of air-conditioning units (Ackerman and Stanton 2008). The energy-saving potential was estimated as 10%–40% in building systems that have high energy efficiency for cooling. Hence, it is significant and urgent to enhance energy efficiency in building systems to reduce energy demand (Saffari et al. 2017).

One approach to enhance energy efficiency in building systems for heating/cooling is using thermal energy storage materials that can serve as a thermal energy reservoir (Saffari et al. 2017), absorbing heat when there is a surplus and releasing heat when there is a deficit. Among different thermal energy storage materials, phase change materials (PCMs) provide an elegant, realistic, and inexpensive solution for temperature management due to their intrinsic thermal properties (Jeong et al. 2019; Frazzica et al. 2019; Zhang et al. 2020; Li and Shi 2019). Proper use of a PCM can minimize the peak heating/cooling loads and has the capability to keep the indoor temperature within a comfort range due to smaller temperature fluctuations, consequently reducing energy consumption in buildings. The room-temperature PCMs have been directly integrated into building materials (Alqallaf and Alawadhi 2013; Ram et al. 2020; Royon et al. 2013). It was reported that by incorporating a PCM, the interior temperature at the room center was reduced by 5°C, and the annual greenhouse gas emission was decreased by 465 kg (Memon et al. 2015a). Also, energy savings from 17% up to 87% (for ideal cases) may be realized (Dincer and Rosen 2001; Stritih and Butala 2011).

Therefore, extensive research has been conducted to optimize the energy efficiency of concrete by incorporating PCMs for storing heat in building constructions (Hunger et al. 2009; Dehdezi et al. 2013; Lecompte et al. 2015; Jayalath et al. 2016). However, PCMs also have some negative impacts on the properties of fresh and hardened concrete that depend on the type and the method of PCM incorporation during the production of the PCM-concrete composite (Cao et al. 2017; Navarro et al. 2016). In addition, the methods of PCM incorporation in concrete compromised the heat storage capacity of the PCM. Existing research primarily focuses on using a solid–liquid PCM, such as paraffin and hydrated salts, which involve a solid–liquid phase change at their transition temperatures (Yeon 2020; Sarı 2004). However, liquid PCMs have high potential of leaking during the solid–liquid phase change (Kasaeian et al. 2017; Hunger et al. 2009). Attempts have been made to incorporate solid–liquid PCMs into concrete by encapsulation, including macroencapsulation and microencapsulation (Jayalath et al. 2016). In microencapsulation, PCMs are packed

[1]Research Assistant, Dept. of Civil, Environmental and Ocean Engineering, Stevens Institute of Technology, 614 River Terrace, Hoboken, NJ 07030. ORCID: https://orcid.org/0000-0002-2115-7272. Email: zliu111@stevens.edu

[2]Research Assistant, Dept. of Civil, Environmental and Ocean Engineering, Stevens Institute of Technology, 614 River Terrace, Hoboken, NJ 07030. Email: jdu18@stevens.edu

[3]Research Assistant, Dept. of Nuclear Engineering, Missouri Univ. of Science and Technology, 301 W 14th St., Rolla, MO 65409. Email: rpsmb7@mst.edu

[4]Associate Professor, Dept. of Nuclear Engineering, Missouri Univ. of Science and Technology, 301 W 14th St., Rolla, MO 65409. Email: schlegelj@mst.edu

[5]Professor, Dept. of Civil, Architectural and Environmental Engineering, Missouri Univ. of Science and Technology, 500 W 16th St., Rolla, MO 65409. Email: khayatk@mst.edu

[6]Assistant Professor, Dept. of Civil, Environmental and Ocean Engineering, Stevens Institute of Technology, 614 River Terrace, Hoboken, NJ 07030 (corresponding author). Email: weina.meng@stevens.edu

Note. This manuscript was submitted on November 3, 2022; approved on April 18, 2023; published online on September 5, 2023. Discussion period open until February 5, 2024; separate discussions must be submitted for individual papers. This paper is part of the ***Journal of Materials in Civil Engineering***, © ASCE, ISSN 0899-1561.

in capsules from less than 1 μm to hundreds of micrometers in size. The microcapsule consists of a PCM core and a shell that is usually made of polymer or silica and fabricated through a physical or chemical process. Microencapsulation has been considered one of the best solutions of preventing leakage of PCMs, and advantageous over the macroencapsulation because of the higher heat transfer rate associated with the reduced size of capsules (Pilehvar et al. 2017; Su et al. 2015). In macroencapsulation, PCMs are impregnated into porous supporting materials with the size greater than 10 mm such as diatomite (Costa et al. 2020), vermiculite (Wen et al. 2017), expanded perlite (Hasanabadi et al. 2019), and expanded graphite (Bi et al. 2021). The primary drawback of macroencapsulation is the low charging/discharging efficiency due to the low thermal conductivity of the PCM and size of the containers (Memon et al. 2015a, b; Cui et al. 2015, 2017; Shi et al. 2014), and the latent heat of the PCMs is compromised significantly because the retention capacity of the porous supporting materials for PCMs is low, normally 30%–60% (Memon 2014). In addition, there is still leakage risk when the supporting materials are overimpregnated with PCMs (Zhang et al. 2021). However, both the macro- and microcapsules are susceptible to damages of the shell. Once the shell is damaged, leakage of PCM will occur and affect the mechanical and thermal properties of concrete (Shen et al. 2021; Niall et al. 2017; Kenisarin and Mahkamov 2007). Damage to the shell may be induced by mechanical and/or other effects during construction and operation, such as impacts of aggregates in mixing, concrete cracks in operation, degradation of shell material, elevated temperature, and so on. The potential to damage the shell is compounded because conventional concrete lacks flowability (Essid et al. 2022; Bao et al. 2022). Additional mechanical vibration is needed to consolidate concrete during construction of building structures. The use of vibration increases the probability of damaging the shell of capsules during construction (Sarbu and Sebarchievici 2018; Lin et al. 2018; Sata et al. 2012). In addition, the charging/discharging efficiency of the encapsulated PCM depends on the heat transfer between concrete and the PCM through the shell. There is a tradeoff between the shell mechanical strength and the heat transfer efficiency (Kroehong et al. 2011; Nie et al. 2017; Song et al. 2022). Heat transfer efficiency may be further reduced by debonding between the shells and surrounding concrete.

Considering these issues, a novel solid–gel PCM has been developed by the author using a eutectic mixture of lauric acid, a fatty acid, and methyl palmitate (a methyl ester) (Saeed et al. 2017). This PCM was modified through the addition of a gelling agent. The gelling agent stabilizes the liquid phase, leading to a form stable solid–gel phase transition. This novel PCM will not leak in the cement-based composite and does not compromise its latent heat. The resulting mixture has a melting temperature of 24.1°C and a latent heat of about 178 J/g, which is much higher than normal form-stable PCMs. Volume expansion during phase change is 3%, which is feasible for incorporation in structural concrete with consideration of the internal stresses induced by volume expansion. The gelling agent also prevents supercooling, which is a common problem with organic PCMs, leading to significantly lower freezing temperatures than melting temperatures. The gelling agent suppresses supercooling by providing freezing nucleation sites within the PCM. Most importantly, the novel PCM is form-stable and so will not leak as solid–liquid PCMs do. This is particularly desirable in building envelope applications; this new PCM does not require encapsulation. Because of this, we envision that (1) the PCM–concrete mass ratio can be higher, leading to larger thermal absorption capacity at a given structural strength, or (2) the PCM–concrete mass ratio can be lower, leading to higher structural strength at a given thermal absorption capacity.

Despite the promise of the novel form-stable solid–gel PCM for enhancing energy efficiency in buildings, knowledge gaps remain and must be addressed. First, a holistic understanding of the effect of the PCM on the fresh and hardened properties of concrete is missing. The use of the PCM may affect the mechanical properties and long-term durability of concrete through changing the hydration kinetics of cementitious materials and the microstructure of hardened concrete. There are several possible mechanisms, such as (1) the PCM fillers may modify the packing density of concrete, (2) the PCM particles provide surfaces that may serve as nucleation sites for precipitation of hydration products in concrete, (3) the surface activity of PCM particles may involve interactions with water and admixtures in concrete, and (4) the volume change of PCM during phase change may induce internal stresses and accelerate degradation of the concrete matrix. There is no experimental data available to help predict the fresh and hardened properties and durability of the form-stable PCM-doped cementitious composite. Furthermore, the PCM will change the thermal properties of concrete, such as the thermal conductivity, specific heat, and so on. This is the basis of enhancing the energy efficiency of buildings. However, fundamental knowledge on the effect of the new solid–gel PCM on the thermal properties of concrete is missing.

This paper aims to investigate the effect of the novel solid–gel PCM on the key properties of cement-based materials including the mini-slump flow, 28-day compressive strength, and modulus of elasticity. In addition, hydration kinetics of mixtures incorporated with PCMs were explored, energy storage capacity of the mixtures was measured, thermal conductivity was obtained using a theoretical model, and the microstructures were analyzed. Finally, the results of thermal properties were used in simulations by EnergyPlus to find out the energy efficiency of the building envelopes built with walls containing this novel PCM. Other parameters that affect the energy efficiency, such as melting point and the outdoor temperatures, were also investigated in the simulations, which can facilitate the optimization of materials design of cement-based materials with PCM for improving energy efficiency of building systems.

Materials and Experimental Program

In this study, the solid–gel PCM is first synthesized and prepared. Then it is used for preparation of different mortar mixtures, which are characterized regarding fresh and hardened properties, microstructure, and thermal properties. Finally, the thermal properties are used to simulate the energy efficiency of building using the PCM-mortar. The structure of the investigation is shown in Fig. 1.

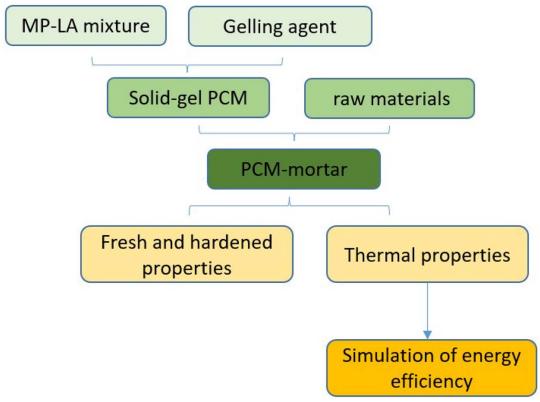

Fig. 1. Flowchart of the investigations on PCM-mortar.

Table 1. The chemical and physical data of solid–gel PCM

Name	Scientific name	Purity (%)	Molecular weight (g/mol)	CAS number	Molecular formula
Methyl palmitate (MP)	Methyl hexadecanoate	99	270.4507	112-39-0	$C_{17}H_{34}O_2$
Lauric acid (LA)	Dodecanoic acid	99	200.3178	143-07-7	$C_{12}H_{24}O_2$

Table 2. The chemical data of the gelling agent

Scientific name (CA index name)	Supplier/product name	Physical form	CAS number
2-hydroxypropyl ether cellulose (HPEC)	Ashland/Klucel-G	Powder	9004-64-2

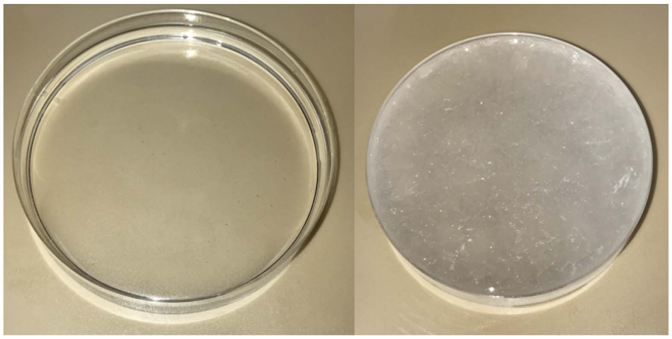

Fig. 2. (a) Digital photograph of the eutectic PCM mixture (MP-LA); and (b) digital photograph of form-stable gelled PCM (MP-LA/HPEC).

Raw Materials

In this study, a eutectic mixture of methyl palmitate and lauric acid (MP-LA) was used as the phase change material. The chemical data for each component are listed in Table 1. The gelling agent was 2-hydroxypropyl ether cellulose (HPEC), with chemical data listed in Table 2. The binary eutectic was prepared as a 60:40 molar ratio of MP to LA. The HPEC gelling agent was then added to the MP-LA mixture with a mass fraction of 10%. Fig. 1 shows a photograph of the "liquid-state" PCM with and without the gelling agent. Fig. 2(a) shows a clear liquid, while Fig. 2(b) shows a waxy semisolid.

Thermal performance of the resulting MP-LA/HPEC mixture is summarized in Table 3. The thermal analysis by differential scanning calorimetry (DSC) shows that the addition of HPEC gelling agent did not cause any phase separation or incongruent melting. The form-stable PCM shows a melting temperature at 24.06°C and a latent heat of 177.9 J/g. In over 30,000 phase change cycles, representing about 80 years of daily thermal cycling, the PCM showed a drift of only 1°C in melting temperature and 2.9% for latent heat of fusion.

To prepare the PCM for the cement-based materials, the PCM was ground into 200-μm-sized grains. Due to the consistency of the material and the material's melting point being only slightly higher than the room temperature, the smaller PCM pieces were mixed with liquid nitrogen immediately before grinding, and the grinder was kept in a 0°C freezer until grinding occurred. This was done to prevent the PCM from melting into a partially solid gel that would build up inside the grinder, because the grinder would heat up as the grinding occurred. Following the grinding, the material was stored in containers in the 0°C freezer until mixing occurred. Type I/II portland cement, class C fly ash (FAC), silica fume (SF), and well-graded river sand were used to produce the mortar mixtures. The chemical compositions and physical characteristics of these raw materials are listed in Table 4. The particle size distribution of the river sand is shown in Fig. 3. The water absorption value of river sand was measured to be 0.14%, in accordance with ASTM C128 (ASTM 2023).

Mixture Design

In this study, 12 mortar mixtures were investigated, with three different water–bind ratios (w/b) and four different PCM contents. All the mixture proportions are presented in Table 5. Each designation for a mixture consists of two components representing w/b and the PCM content. For example, the designation W35-P20 represents the mixture with a w/b of 0.35 and 20% of sand replaced by PCM.

Heat of Hydration

The rate and extent of hydration were monitored using an isothermal conduction calorimeter (Calmetrix I-CAL 8000), which was programmed to maintain the sample at a constant temperature of 20°C ± 0.1°C. About 75 g of fresh mixture was sealed in a plastic vial and placed into the calorimeter. The heat of hydration data was continuously measured from 2 min after completion of mixing the mortar and continued for 36 h. The calorimetry results were normalized by mass of the binder.

Fresh and Mechanical Properties

The unit weight and mini-slump flow values of fresh mixtures were measured in accordance with ASTM C138 and ASTM C230/C230M (ASTM 2017a), respectively. Compressive strength at 28 days was evaluated using 50-mm cubes according to ASTM C109 (ASTM 2020). The Young's modulus at 28 days was evaluated in accordance with ASTM C469 (ASTM 2017b). Three sample replicates were prepared for each test. The average results are reported.

Thermal Properties

A Seiko DSC 6200 calorimeter was used to measure the melting temperatures, specific heats, and latent heats of the mixtures. Samples were tested using aluminum sample pans and lids. The calorimetric precision, sensitivity, and temperature accuracy is within ±1%, 1 μW, and ±0.05°C respectively.

Because the thermal conductivity of each component in the mortar is available and multiple models have been verified to effectively

Table 3. DSC data for gelled Eutectic PCM

PCM name	T_m (°C)	T_f (°C)	ΔH_m (J/g)	ΔH_f (J/g)	C_p^{solid} (W/mK)	C_p^{melted} (W/mK)	ρ^{solid} (g/mL)	ρ^{melted} (g/mL)
MP-LA/HPEC	24.1	20.8	177.9	176.4	1.89	2.88	0.893	0.847

Note: T_m is melting temperature, T_f is freezing temperature, ΔH_m is melting enthalpy, ΔH_f is freezing enthalpy, C_p^{solid} is solid thermal conductivity, C_p^{melted} is melted thermal conductivity, ρ^{solid} is solid density, and ρ^{melted} is melted density.

Table 4. Chemical and physical properties of the cementitious materials and sand

Composition	Type I/II cement	Class C fly ash	Silica fume	River sand
SiO_2 (%)	19.8	36.50	95.50	80.30
Al_2O_3 (%)	4.5	24.80	0.70	10.50
Fe_2O_3 (%)	3.2	5.20	0.30	3.43
CaO (%)	64.2	28.10	0.40	1.72
MgO (%)	2.7	5.00	0.50	1.70
SO_3 (%)	3.4	2.50	—	1.07
Na_2O eq. (%)	—	—	0.40	—
C_3S (%)	61	—	—	—
C_2S (%)	8	—	—	—
C_3A (%)	6	—	—	—
C_4AF (%)	8.40	—	—	—
Loss of ignition (%)	2.6	0.50	2.00	1.28
Blaine surface area (m^2/kg)	379	—	—	—
B.E.T specific area (m^2/kg)	—	—	18,200	—
Specific gravity, SSD	3.15	2.70	2.20	2.65

Note: B.E.T = Brunauer, Emmett, and Teller.

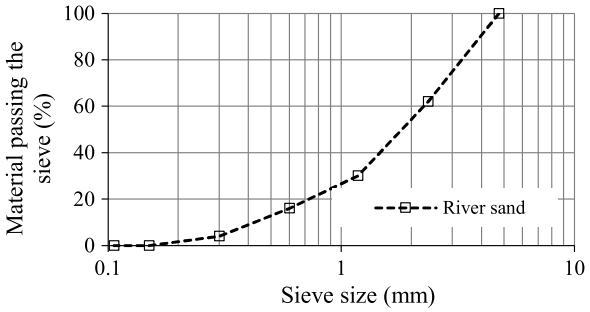

Fig. 3. The particle size distribution of the river sand.

Table 5. Mixture design of the investigated mixtures (unit: kg/m^3)

#	Designations	w/b	PCM	SF	FAC	Cement	River sand	Water
1	W35-P0	0.35	0.0	36.4	357.6	571.9	902.1	310.4
2	W35-P10	0.35	33.4	36.4	357.6	571.9	811.9	310.4
3	W35-P20	0.35	66.9	36.4	357.6	571.9	721.7	310.4
4	W35-P30	0.35	100.3	36.4	357.6	571.9	631.5	310.4
5	W45-P0	0.45	0.0	33.1	325.3	520.2	820.6	372.7
6	W45-P10	0.45	30.4	33.1	325.3	520.2	716.2	372.7
7	W45-P20	0.45	60.8	33.1	325.3	520.2	636.6	372.7
8	W45-P30	0.45	91.3	33.1	325.3	520.2	557.0	372.7
9	W55-P0	0.55	0.0	30.5	299.2	478.4	754.7	423.1
10	W55-P10	0.55	28.0	30.5	299.2	478.4	679.2	423.1
11	W55-P20	0.55	56.0	30.5	299.2	478.4	603.7	423.1
12	W55-P30	0.55	83.9	30.5	299.2	478.4	528.3	423.1

predict the thermal conductivity of concrete (Lee et al. 2006; Mandilaras et al. 2015; Wang et al. 2006; Meshgin and Xi 2013), in this paper, the thermal conductivity will be obtained using one of these models, the generalized self-consistent model (GSC) that has been proved highly effective in multiple studies (Lee et al. 2006; Meshgin and Xi 2013).

SEM Observations

Small pieces from fractured mortar specimens were taken as samples for scanning electron microscope (SEM) analysis. Before examination, the broken pieces were rinsed using 99.8% isopropyl alcohol, oven dried at 50°C for 24 h, and then coated with a very thin layer of gold for conduction. Three images per sample were taken using the SEM with backscattered electron mode.

Key Properties of PCM-Mortar

Fresh and Mechanical Properties

Fig. 4(a) shows the mini-slump results of tested samples. With the increase of PCM content from 0% to 30%, the mini-slump spreads of mixtures with a w/b of 0.35, 0.45, and 0.55 decreased by 58%, 57%, and 26%, respectively. This is because the replacement of sand by PCM particles introduced more surface area for water absorption, decreased the free water in mixtures, and hence minimized the workability. When w/b increases and reaches 0.55, due to more free water introduced to the mixture, the impact of the PCM was offset significantly and the reduction in mini-slump was mitigated.

Fig. 4(b) presents the results of 28-day compressive strength, and it was found that increasing PCM content from 0% to 30% led to reduction of compressive strength by 48%, 50%, and 64%, respectively, for mixtures with a w/b of 0.35, 0.45, and 0.55. This could be because the lack of free water due to the water sequestration by PCM particles hindered the formation of hydration product, which led to decrease in compressive strength (Eddhahak et al. 2014). Also, with the increase of PCM content, there are less sands providing a pozzolanic effect and greater interaction with the cementitious matrix. In addition, sand with greater mechanical strength partially replaced by the polymeric PCM can lead to reduction of compressive strength. Fig. 4(c) gives the results of elastic modulus of tested samples. It showed that when PCM increased from 0% to 30%, elastic modulus of mixtures with a w/b of 0.35, 0.45, and 0.55 decreased by 38%, 40%, and 41%, respectively. This followed the same trend in compressive strength because the elastic modulus and compressive strength are intrinsically related (Haurie et al. 2016). The compressive strength was significantly compromised owing to the incorporation of PCM in the mortar. However, this mortar is designed for building walls. Given the requirement of compressive strength of mortar for building walls is 13.8 MPa according to ASTM C90-22 (ASTM 2022), which is much lower than all mixtures except for W55-P30, the PCM mortar can be safely applied. But for heavily loaded applications, the compressive strength needs to be improved. Further studies will be conducted to enhance the mechanical properties while maintaining the benefits of thermal properties from PCM (e.g., the mix design can be optimized to improve the packing density of the mixtures for higher strength).

Heat of Hydration

Fig. 5 presents the hydration heat flow and cumulative hydration heat of mixtures W45P0, W45P10, W45P20, and W45P30. At the same w/b of 0.45, with the increase of PCM content from 0% to 30%, the hydration peak is reduced from 3.62 to 3.07 mW/g (by 15%), the time reaching the peak remained the same at around 12 h for all mixtures. This is because the replacement of sand by PCM introduces more surface area for water adsorption, which hindered the formation of hydration product, as a result the heat peak decreased significantly in mixtures with 30% PCM compared with that of mixtures without PCM. This can explain the results that mixtures with PCM resulted in lower hardened properties compared with mixtures without PCM.

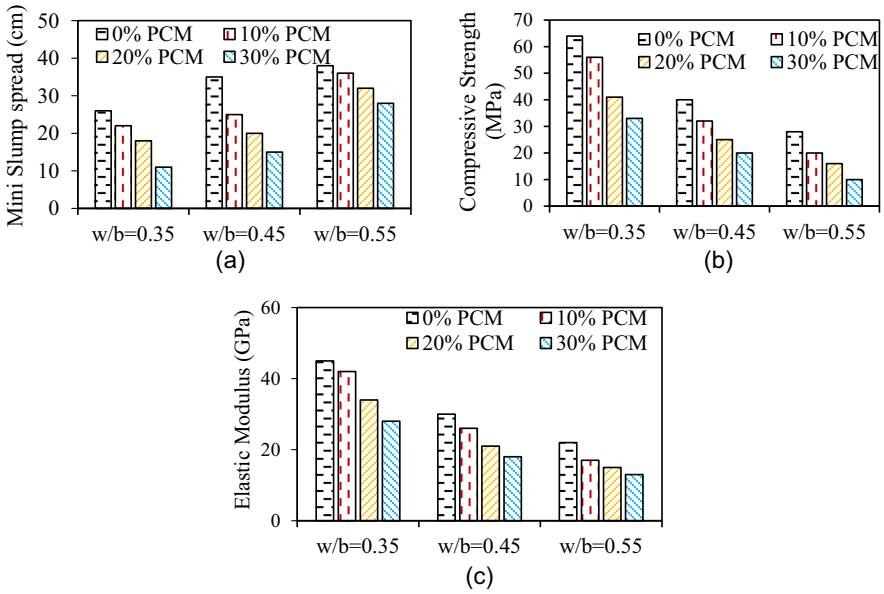

Fig. 4. (a) Mini-slump of mixtures with different w/b and PCM contents; (b) compressive strength at 28 days of mixtures with different w/b and PCM contents; and (c) elastic modulus of mixtures at 28 days of mixtures with different w/b and PCM contents.

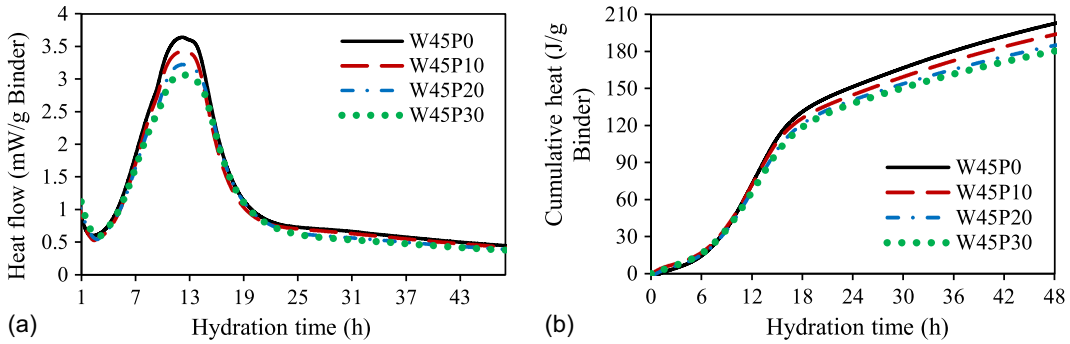

Fig. 5. Effects of PCM on hydration heat: (a) heat flow; and (b) cumulative heat.

Thermal Properties

Energy Storage Capacity

The energy storage curves are presented in Fig. 6. For mixtures with the same w/b, increase of PCM content can effectively enhance the energy storage capacity over the temperature range from 24°C to 30°C due to the phase change process of PCM. The melting temperature point of investigated mixtures was not considerably affected by variations of w/b and PCM contents. The mixture W45-P30 achieved the highest latent heat value (i.e., over 7 J/g). However, given the latent heat of 178 J/g in pure PCM, a latent heat of about 8 J/g was expected for W45-P30 mixture. The less measured latent heat indicates that there may be some additional interactions occurring during the mixing and curing process. Further research is necessary to understand the chemical and physical mechanisms.

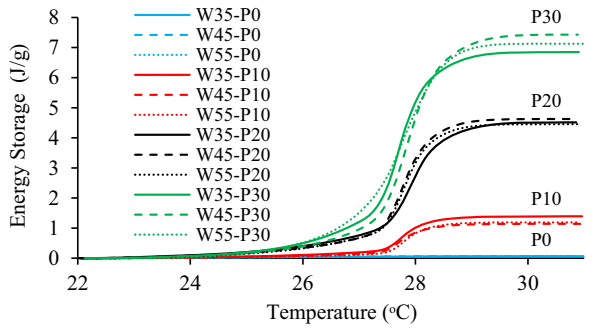

Fig. 6. Energy storage of mixtures with various w/b and PCM contents.

Thermal Conductivity

In this paper, the GSC model (Meshgin and Xi 2013) was used to determine the thermal conductivity of mortar with PCM. This model was developed as a "Three Phase Model" in which the matrix and the inclusions are two constituent phases, and the composite is the third one. The spherical inclusion of with a radius a is embedded in a concentric sphere matrix with a of radius b, which is embedded in an effective media as is shown in Fig. 7(a). According to the steady-state conduction and equation of this composite, as well as the continuity conditions of the heat flux satisfied at the boundaries between the inclusion and the matrix, the effective thermal conductivity can be derived and calculated as

J. Mater. Civ. Eng., 2023, 35(11): 04023425

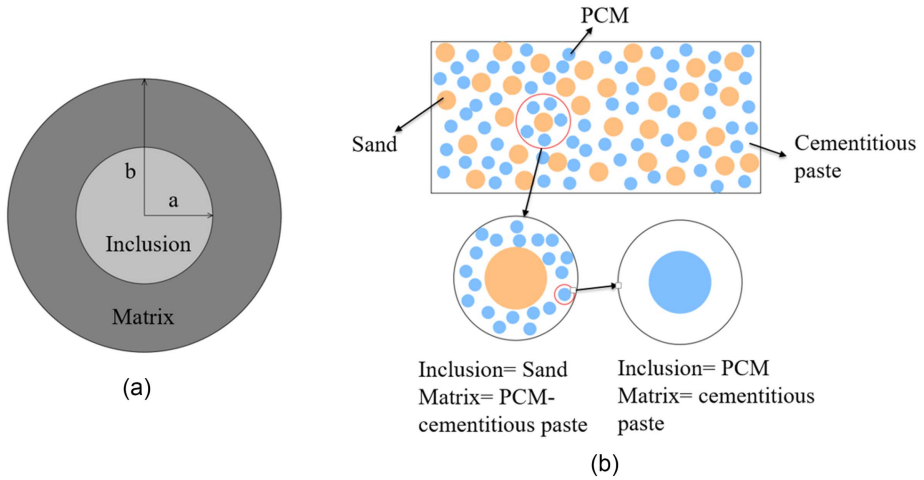

Fig. 7. (a) Modeling of PCM-mortar: the generalized self-consistent model; and (b) modeling of PCM-mortar: multiscale modeling of the composite.

$$K_{\text{eff}} = K_m \left[1 + \frac{c}{\frac{1-c}{3} + \frac{K_m}{K_i - K_m}} \right] \tag{1}$$

where $c = (a/b)^3$ is the function of radius ratio of the inclusions and K_i and K_m are the conductivity of the inclusion and matrix.

Fig. 7(b) shows a schematic view of the multiscale model for the PCM-incorporated mortar. It is shown that PCM-mortar has three different phases: sand, PCM particles, and cementitious paste. At largest scale, PCM-mortar can be considered as a two-phase composite with sand as the inclusion and PCM-cementitious paste as the matrix. Likewise, the PCM-cementitious paste can be considered as a two-phase composite with PCM as the inclusion and cementitious paste as the matrix.

Thermal properties of phases are listed in Table 6. According to the GSC model for PCM-mortar and Eq. (1), the thermal conductivity of mixtures with PCM content from 0% to 30% can be obtained, and the results are shown in Fig. 8. The results indicate that increasing the PCM content can significantly decrease the thermal conductivity of PCM-mortar. Because the lower thermal conductivity can prevent indoor heat exchanging with outside of the building envelopes, it will be beneficial to maintain a more stable temperature and improve energy efficiency.

Table 6. Thermal conductivity of phases in PCM-mortar

Composition	PCM	Sand	Cementitious paste
Conductivity [W/(m K)]	0.18	3.0	0.75

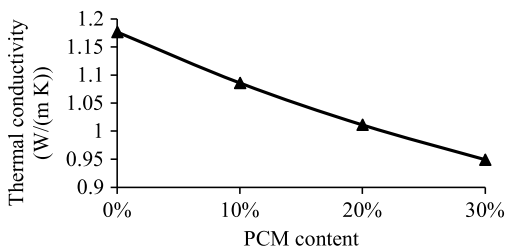

Fig. 8. GSC model-based thermal conductivity of mixtures with different PCM content.

SEM Observations

The results of microstructure analysis by SEM are shown in Fig. 9. With the same w/b, the 30% PCM incorporated mortar has an obviously larger thickness of interfacial transition zone (ITZ) than that of the mixture without PCM. And the paste matrix in mixture with PCM is apparently more porous than that of mixture without PCM. These could result from: (1) the free water was adsorbed on the surface of PCM; hence, hydration products are decreased due to the reduction of free water and more pores are unfilled; and (2) incompatibility between PCM particles and cementitious matrix resulted in weakened interface between them. These can explain the reduction in compressive strength and modulus of elasticity of mixtures with the increased content of PCM.

Energy Efficiency of Buildings Using PCM-Mortar

Numerical simulations were conducted to investigate the energy efficiency of building envelopes with and without PCM incorporated. The key parameters of PCM properties used in the models were also explored to enhance the understanding of optimization of PCM-mortar.

Numerical Model

The numerical simulation was conducted using EnergyPlus 9.1, which is a program specialized for modeling building energy consumption. As is shown in Fig. 10, the building with dimensions of $10 \times 5 \times 5$ m was built as the building model to represent the practice of a residential house. The walls on the four sides are constructed with PCM-mortar inside to investigate their effect on energy efficiency of the whole building. Fig. 13 presents the structure of the walls. There are four layers in the structure: 1.3-cm (0.5-in.) stucco, 20.3-cm (8-in.) PCM-mortar, 5-cm (2-in.) insulation, and 1.3-cm (0.5-in.) gypsum from outdoor to indoor.

Modeling Inputs

PCM Properties

In EnergyPlus, the one-dimensional Conduction Finite-difference (CondFD) solution algorithm is introduced to simulate the phase change process. This algorithm uses an implicit finite difference scheme coupled with an enthalpy–temperature function to calculate phase change energy accurately (Wang et al. 2020).

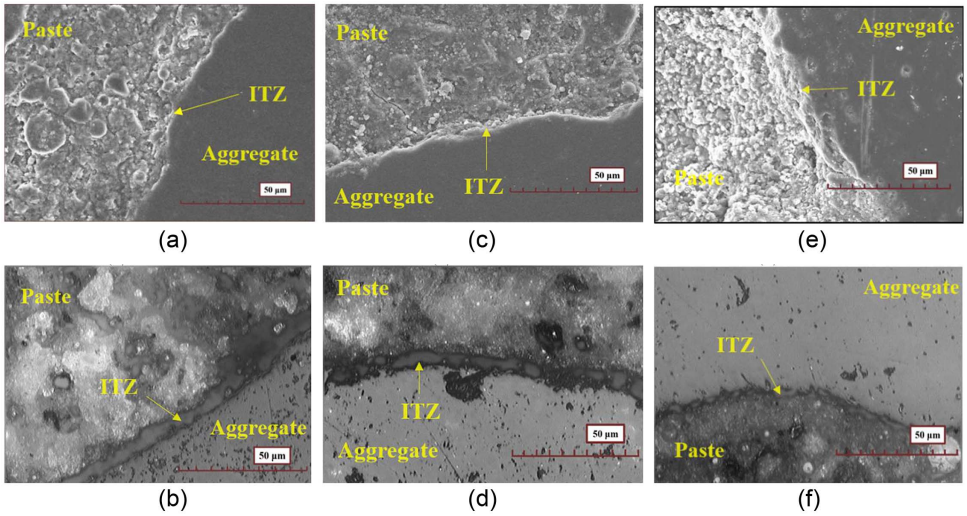

Fig. 9. Microscopic morphology of ITZ under different w/b and PCM content: (a) W35P0; (b) W35P30; (c) W45P0; (d) W45P30; (e) W55P0; and (f) W55P30.

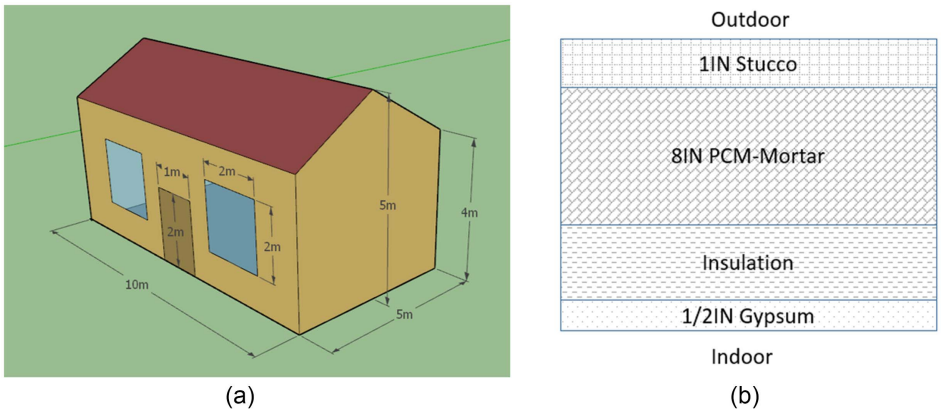

Fig. 10. (a) Modelling of building energy consumption: building model simulated in EnergyPlus; and (b) the structure of walls in the building model.

In EnergyPlus, enthalpy under different temperatures of the simulated PCM are input. The enthalpy–temperature curves obtained from test results of aforementioned mixtures W45-P0, W45-P10, W45-P20, and W45-P30, abbreviated as NonPCM, P10, P20, and P30 here, are set as the PCM properties of the PCM-mortar in the walls separately to compare their effects on the simulations. Fig. 11 shows the enthalpy–temperature function of the PCM-mortar simulated.

Weather Conditions and Indoor Temperature

The EPW (EnergyPlus Weather Format) file of City 1 was used in the simulation. Fig. 12 shows the variation of outdoor temperature in a whole year. The climate has distinct four seasons with the hottest weather in June and July and the coldest weather in December and January.

To remain a comfortable indoor air temperature, the thermostat was set with a cooling set point temperature of 22°C and a heating

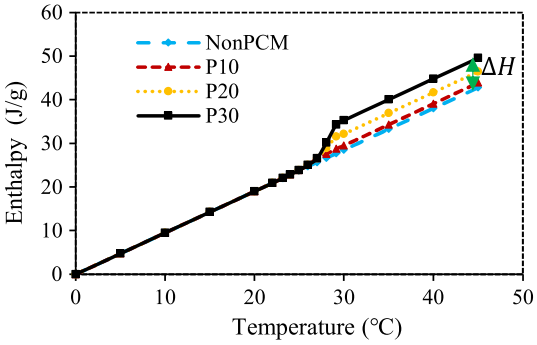

Fig. 11. Enthalpy–temperature function of PCM-mortar.

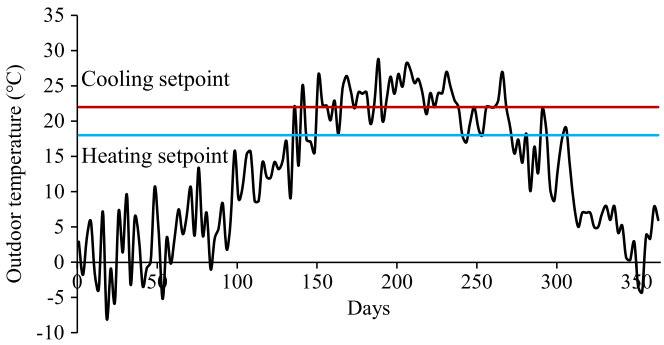

Fig. 12. The annual outdoor temperature variation in City 1.

J. Mater. Civ. Eng., 2023, 35(11): 04023425

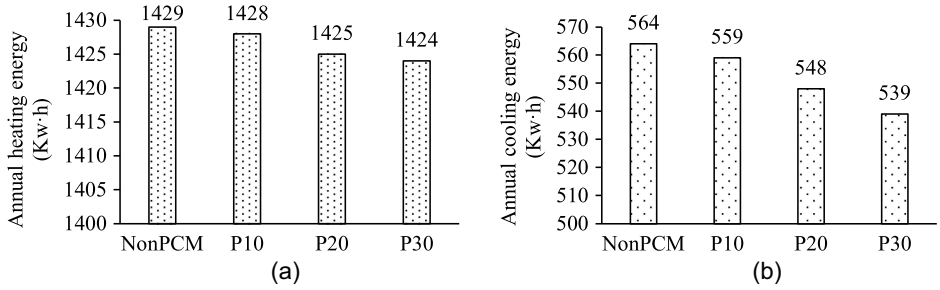

Fig. 13. Annual heating and cooling energy consumption: (a) heating energy; and (b) cooling energy.

set point temperature of 18°C. Hence, the indoor temperature was maintained between 18°C and 22°C.

Energy Efficiency Simulation Results

Energy Consumption

Fig. 13 presents the 1-year energy consumption in total in terms of the heating and cooling. It can be found that both heating and cooling energy consumption decreased with the increase of PCM content in the walls. Specifically, P30 building can save 5% energy consumption for cooling compared with the NonPCM reference.

This is because in hot weather, the PCM wall can transfer some absorbed energy to latent heat in PCM and conduct less heat to indoor space, thus the heating, ventilation, and air conditioning (HVAC) system need less cooling energy to maintain indoor temperature. Likewise, the HVAC system needs less heating energy to prevent indoor temperature from falling in cold weather. Noteworthy, the energy saving for cooling is more significant than that for heating; this could be the result of the high melting temperature of PCM-mortar, which makes it less possible to have phase change process in cold weather.

Electricity Load

Electricity load, which represents the electric power required from the supply, can be used to evaluate the energy demand in terms of the heating and cooling system in the simulations. Fig. 14 gives the cooling loads for 48 h from August 9 to 10, which are two typical hot days in summer. It is shown that cooling load is considerably reduced with the increase of PCM in the wall. The areas of the curves which represent the energy consumption for cooling show that PCM-incorporated walls are beneficial for reducing cooling energy consumption. Furthermore, for the P30 building, peak cooling load is reduced by about 12% on August 9 and 8% on August 10 compared with the NonPCM building. Thus, it can be indicated that PCM walls can minimize both the peak demand and total demand of electricity supply, which will mitigate the difficulties for electric companies because their electricity generation capacity must meet the peak demand and the total demand.

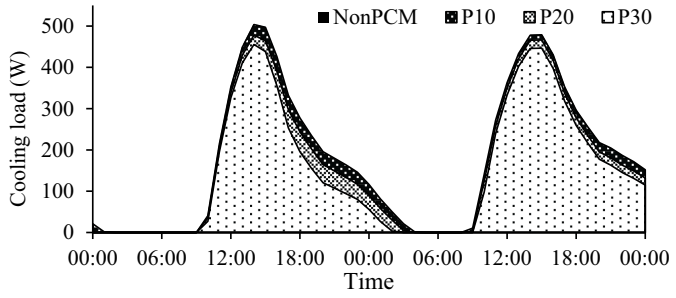

Fig. 14. Cooling load from August 9 to 10.

Parameters Affecting the Energy Efficiency

Weather

Weather has an important effect on the efficiency of the functionality of PCM walls because it directly affects the degree and frequency of phase change process happening in the PCM walls. Therefore, three different types of weather in City 1, City 2, and City 3 are compared in the simulation. Fig. 15 presents the annual outdoor temperature variation in these three cities. It can be seen that, compared with City 1, the temperature in City 2 on summer days is higher and more variable while the temperature in City 3 is lower and more stable.

Fig. 16 compares the cooling energy saving amount and percentage in PCM buildings compared with their NonPCM references. It was found that, compared with City 2, both the amount and

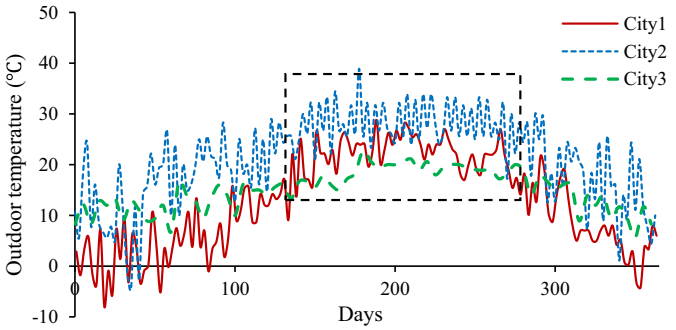

Fig. 15. Annual outdoor temperature of City 1, City 2, and City 3.

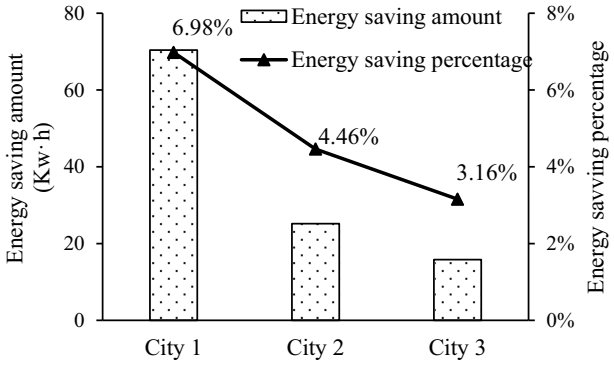

Fig. 16. Cooling energy saving under different weathers of three cities with three types of weather.

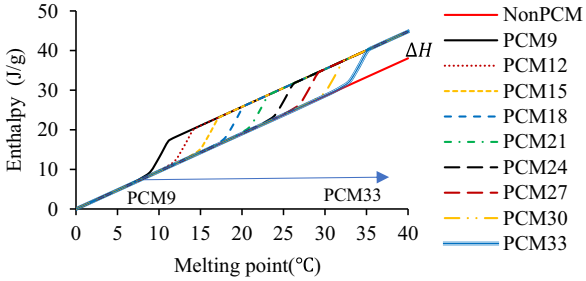

Fig. 17. Enthalpy–temperature function of PCM mortar with different melting points.

percentage of energy saving for cooling in City 1 are higher while both are lower in City 3. This is possibly because high temperature makes it more possible for melting to happen and more fluctuating temperatures make the phase change happen more frequently. Thus, it can be indicated that the PCM can be more effective in increasing energy efficiency of building in a relatively high and more fluctuant temperature environment.

Melting Point of PCM

Another important parameter that affects energy consumption is the melting point of the PCM because it decides the starting point of latent heat storage and influences the total heat transfer under given climate data. If the melting point is too high above or too low below the outdoor temperature, it will be difficult for the phase change process to happen.

Figs. 17(a–c) present the PCM properties of different PCM mortar with melting points from 9 to 33°C, and they are applied in the simulation and their effect on energy consumption is investigated.

Fig. 18 gives the annual heating and cooling energy consumed in simulated PCM buildings and the NonPCM references. As is shown in Fig. 17(a), it is indicated that the melting point above 33°C contributes negligibly to heating energy saving. And contribution of the melting point below 15°C to cooling energy saving is also ignorable according to Fig. 17(b). The 18°C and 27°C are the optimal melting temperatures that contribute to the best energy saving performance for heating and cooling separately, depicted in Fig. 17(c). The optimal PCM that leads to the least total energy consumption has a melting temperature between 21°C and 27°C. Thus, it can be indicated a reasonable range of melting points should be considered according to the weather conditions used to obtain a better energy-saving performance of the building envelope.

Conclusions

In this study, the main findings from experimental studies and numeral simulations are summarized:

1. Energy storage capacity of the cement-based materials increases as the increase of PCM content. A 30% replacement of sand by PCM can increase the latent heat of the mixture to 7 J/g.
2. Fresh and mechanical properties of the mixtures were highly impacted by the addition of the PCM. The workability was reduced with the increase of PCM. The 28-day compressive strength and elastic modulus also decreased significantly with the increase of PCM.
3. Simulation results demonstrated that PCM-mortar are beneficial for reducing energy consumption and electricity load in terms of heating and cooling. Thirty percent PCM-incorporated walls can contribute to 5% energy saving for cooling in a whole year and 12% reduction in peak cooling load.

This study is a feasibility study on utilization of the novel PCM-mortar in cementitious materials for enhancing energy efficiency of building envelopes. It fills the blank of understanding on how this solid–gel PCM influences key properties of cementitious materials and energy efficiency of building envelopes. Further studies need to be carried out to understand the fundamentals on how PCMs interact with cementitious matrix, which will give more in-depth understanding on how to design the solid–gel PCM composite and the cementitious mixtures in different applications. In addition, more experimental studies need to be conducted to verify the durability and volume stability of PCM-incorporated cementitious materials for further expansion of the applications of this material.

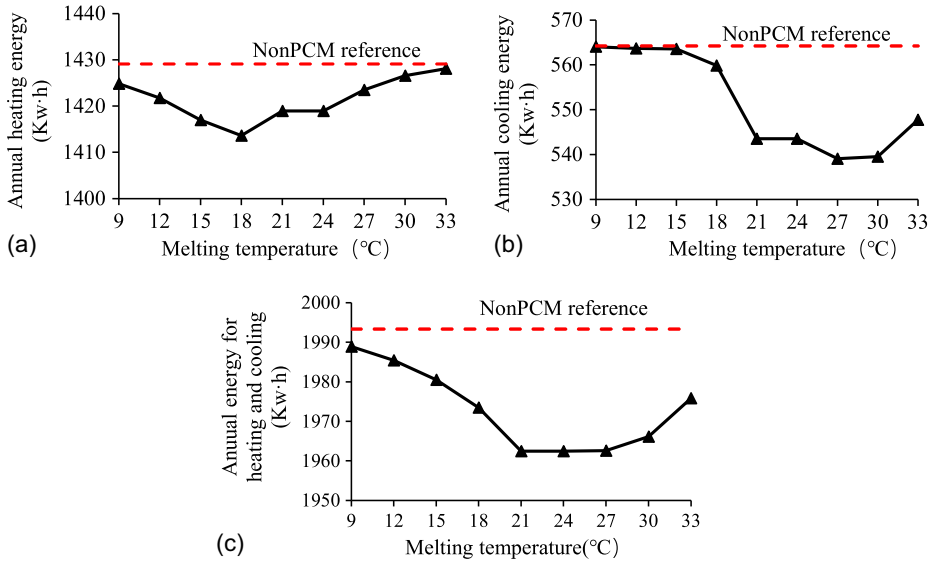

Fig. 18. Annual heating and cooling energy consumed in 1 year: 18°C and 27°C are the optimal melting temperature for PCM to achieve lowest heating and cooling energy consumption respectively, and 21°C–27°C contributes to the highest total energy saving: (a) heating energy; (b) cooling energy; and (c) total energy for heating and cooling.

Data Availability Statement

All data, models, and code generated or used during the study appear in the published paper.

Acknowledgments

This research was partially funded by National Science and Foundation (Award No. CMMI 2046407) and New Jersey Department of Transportation [Task Order 349—Bridge Resource Program (2017–2020), contract ID No. 17-60139, Federal Project No. D00S237].

References

Ackerman, F., and E. A. Stanton. 2008. *The cost of climate change*. New York: Natural Resources Defense Council.

Alqallaf, H. J., and E. M. Alawadhi. 2013. "Concrete roof with cylindrical holes containing PCM to reduce the heat gain." *Energy Build.* 61 (Jun): 73–80. https://doi.org/10.1016/j.enbuild.2013.01.041.

ASTM. 2017a. *Standard specification for flow table for use in tests of hydraulic cement*. ASTM C230/C230M. West Conshohocken, PA: ASTM.

ASTM. 2017b. *Standard test method for static modulus of elasticity and Poisson's ratio of concrete in compression*. ASTM C469-02. West Conshohocken, PA: ASTM.

ASTM. 2020. *Standard test method for compressive strength of hydraulic cement mortars*. ASTM C109. West Conshohocken, PA: ASTM.

ASTM. 2022. *Standard specification for loadbearing concrete masonry units*. ASTM C90-22. West Conshohocken, PA: ASTM.

ASTM. 2023. *Standard test method for relative density (specific gravity) and absorption of fine aggregate*. ASTM C128-22. West Conshohocken, PA: ASTM.

Bao, X., X. Qi, H. Cui, W. Tang, and X. Chen. 2022. "Experimental study on thermal response of a PCM energy pile in unsaturated clay." *Renewable Energy* 185 (Feb): 790–803. https://doi.org/10.1016/j.renene.2021.12.062.

Bi, L., G. Long, C. Ma, J. Wu, and Y. Xie. 2021. "Effect of phase change composites on hydration characteristics of steam-cured cement paste." *Constr. Build. Mater.* 274 (Mar): 122030. https://doi.org/10.1016/j.conbuildmat.2020.122030.

Cao, V. D., S. Pilehvar, C. Salas-Bringas, A. M. Szczotok, J. F. Rodriguez, M. Carmona, N. Al-Manasir, and A. L. Kjøniksen. 2017. "Microencapsulated phase change materials for enhancing the thermal performance of Portland cement concrete and geopolymer concrete for passive building applications." *Energy Convers. Manage.* 133 (Feb): 56–66. https://doi.org/10.1016/j.enconman.2016.11.061.

Costa, J. A. C., A. E. Martinelli, R. M. do Nascimento, and A. M. Mendes. 2020. "Microstructural design and thermal characterization of composite diatomite-vermiculite paraffin-based form-stable PCM for cementitious mortars." *Constr. Build. Mater.* 232 (Jan): 117167. https://doi.org/10.1016/j.conbuildmat.2019.117167.

Cui, H., S. A. Memon, and R. Liu. 2015. "Development, mechanical properties and numerical simulation of macro encapsulated thermal energy storage concrete." *Energy Build.* 96 (Jun): 162–174. https://doi.org/10.1016/j.enbuild.2015.03.014.

Cui, H., W. Tang, Q. Qin, F. Xing, W. Liao, and H. Wen. 2017. "Development of structural-functional integrated energy storage concrete with innovative macro-encapsulated PCM by hollow steel ball." *Appl. Energy* 185 (Jan): 107–118. https://doi.org/10.1016/j.apenergy.2016.10.072.

Dehdezi, P. K., M. R. Hall, A. R. Dawson, and S. P. Casey. 2013. "Thermal, mechanical and microstructural analysis of concrete containing micro-encapsulated phase change materials." *Int. J. Pavement Eng.* 14 (5): 449–462. https://doi.org/10.1080/10298436.2012.716837.

Dincer, I., and M. A. Rosen. 2001. "Energetic, environmental and economic aspects of thermal energy storage systems for cooling capacity." *Appl. Therm. Eng.* 21 (11): 1105–1117. https://doi.org/10.1016/S1359-4311(00)00102-2.

Eddhahak, A., S. Drissi, J. Colin, S. Caré, and J. Neji. 2014. "Effect of phase change materials on the hydration reaction and kinetic of PCM-mortars." *J. Therm. Anal. Calorim.* 117 (2): 537–545. https://doi.org/10.1007/s10973-014-3844-x.

Essid, N., A. Eddhahak, and J. Neji. 2022. "Experimental and numerical analysis of the energy efficiency of PCM concrete wallboards under different thermal scenarios." *J. Build. Eng.* 45 (Jan): 103547. https://doi.org/10.1016/j.jobe.2021.103547.

Frazzica, A., V. Brancato, V. Palomba, D. La Rosa, F. Grungo, L. Calabrese, and E. Proverbio. 2019. "Thermal performance of hybrid cement mortar-PCMs for warm climates application." *Sol. Energy Mater. Sol. Cells* 193 (May): 270–280. https://doi.org/10.1016/j.solmat.2019.01.022.

Hasanabadi, S., S. M. Sadrameli, H. Soheili, H. Moharrami, and M. M. Heyhat. 2019. "A cost-effective form-stable PCM composite with modified paraffin and expanded perlite for thermal energy storage in concrete." *J. Therm. Anal. Calorim.* 136 (3): 1201–1216. https://doi.org/10.1007/s10973-018-7731-8.

Haurie, L., S. Serrano, M. Bosch, A. I. Fernandez, and L. F. Cabeza. 2016. "Single layer mortars with microencapsulated PCM: Study of physical and thermal properties, and fire behaviour." *Energy Build.* 111 (Jan): 393–400. https://doi.org/10.1016/j.enbuild.2015.11.028.

Hunger, M., A. G. Entrop, I. Mandilaras, H. J. Brouwers, and M. Founti. 2009. "The behavior of self-compacting concrete containing micro-encapsulated phase change materials." *Cem. Concr. Compos.* 31 (10): 731–743. https://doi.org/10.1016/j.cemconcomp.2009.08.002.

Jayalath, A., R. San Nicolas, M. Sofi, R. Shanks, T. Ngo, L. Aye, and P. Mendis. 2016. "Properties of cementitious mortar and concrete containing micro-encapsulated phase change materials." *Constr. Build. Mater.* 120 (Sep): 408–417. https://doi.org/10.1016/j.conbuildmat.2016.05.116.

Jeong, S. G., S. Wi, S. J. Chang, J. Lee, and S. Kim. 2019. "An experimental study on applying organic PCMs to gypsum-cement board for improving thermal performance of buildings in different climates." *Energy Build.* 190 (May): 183–194. https://doi.org/10.1016/j.enbuild.2019.02.037.

Kasaeian, A., F. Pourfayaz, E. Khodabandeh, and W. M. Yan. 2017. "Experimental studies on the applications of PCMs and nano-PCMs in buildings: A critical review." *Energy Build.* 154 (Nov): 96–112. https://doi.org/10.1016/j.enbuild.2017.08.037.

Kenisarin, M., and K. Mahkamov. 2007. "Solar energy storage using phase change materials." *Renewable Sustainable Energy Rev.* 11 (9): 1913–1965. https://doi.org/10.1016/j.rser.2006.05.005.

Kroehong, W., T. Sinsiri, and C. Jaturapitakkul. 2011. "Effect of palm oil fuel ash fineness on packing effect and pozzolanic reaction of blended cement paste." *Procedia Eng.* 14 (Jan): 361–369. https://doi.org/10.1016/j.proeng.2011.07.045.

Lecompte, T., P. Le Bideau, P. Glouannec, D. Nortershauser, and S. Le Masson. 2015. "Mechanical and thermo-physical behaviour of concretes and mortars containing phase change material." *Energy Build.* 94 (May): 52–60. https://doi.org/10.1016/j.enbuild.2015.02.044.

Lee, Y. M., R. B. Yang, and S. S. Gau. 2006. "A generalized self-consistent method for calculation of effective thermal conductivity of composites with interfacial contact conductance." *Int. Commun. Heat Mass Transfer* 33 (2): 142–150. https://doi.org/10.1016/j.icheatmasstransfer.2005.10.004.

Li, M., and J. Shi. 2019. "Review on micropore grade inorganic porous medium based form stable composite phase change materials: Preparation, performance improvement and effects on the properties of cement mortar." *Constr. Build. Mater.* 194 (Jan): 287–310. https://doi.org/10.1016/j.conbuildmat.2018.10.222.

Lin, Y., Y. Jia, G. Alva, and G. Fang. 2018. "Review on thermal conductivity enhancement, thermal properties and applications of phase change materials in thermal energy storage." *Renewable Sustainable Energy Rev.* 82 (Feb): 2730–2742. https://doi.org/10.1016/j.rser.2017.10.002.

Mandilaras, I. D., D. A. Kontogeorgos, and M. A. Founti. 2015. "A hybrid methodology for the determination of the effective heat capacity of PCM enhanced building components." *Renewable Energy* 76 (Apr): 790–804. https://doi.org/10.1016/j.renene.2014.11.078.

Memon, S. A. 2014. "Phase change materials integrated in building walls: A state of the art review." *Renewable Sustainable Energy Rev.* 31 (Mar): 870–906. https://doi.org/10.1016/j.rser.2013.12.042.

Memon, S. A., H. Cui, T. Y. Lo, and Q. Li. 2015a. "Development of structural–functional integrated concrete with macro-encapsulated PCM for thermal energy storage." *Appl. Energy* 150 (Jul): 245–257. https://doi.org/10.1016/j.apenergy.2015.03.137.

Memon, S. A., H. X. Cui, H. Zhang, and F. Xing. 2015b. "Utilization of macro encapsulated phase change materials for the development of thermal energy storage and structural lightweight aggregate concrete." *Appl. Energy* 139 (Feb): 43–55. https://doi.org/10.1016/j.apenergy.2014.11.022.

Meshgin, P., and Y. Xi. 2013. "Multi-scale composite models for the effective thermal conductivity of PCM-concrete." *Constr. Build. Mater.* 48 (Nov): 371–378. https://doi.org/10.1016/j.conbuildmat.2013.06.068.

Navarro, L., A. De Gracia, D. Niall, A. Castell, M. Browne, S. J. McCormack, P. Griffiths, and L. F. Cabeza. 2016. "Thermal energy storage in building integrated thermal systems: A review. Part 2. Integration as passive system." *Renewable Energy* 85 (Jan): 1334–1356. https://doi.org/10.1016/j.renene.2015.06.064.

Niall, D., O. Kinnane, R. P. West, and S. McCormack. 2017. "Mechanical and thermal evaluation of different types of PCM–concrete composite panels." *J. Struct. Integrity Maint.* 2 (2): 100–108. https://doi.org/10.1080/24705314.2017.1318039.

Nie, S., S. Hu, F. Wang, C. Hu, X. Li, and Y. Zhu. 2017. "Pozzolanic reaction of lightweight fine aggregate and its influence on the hydration of cement." *Constr. Build. Mater.* 153 (Oct): 165–173. https://doi.org/10.1016/j.conbuildmat.2017.07.111.

Pilehvar, S., V. D. Cao, A. M. Szczotok, L. Valentini, D. Salvioni, M. Magistri, R. Pamies, and A. L. Kjøniksen. 2017. "Mechanical properties and microscale changes of geopolymer concrete and Portland cement concrete containing micro-encapsulated phase change materials." *Cem. Concr. Res.* 100 (Oct): 341–349. https://doi.org/10.1016/j.cemconres.2017.07.012.

Ram, V. V., R. Singhal, and R. Parameshwaran. 2020. "Energy efficient pumpable cement concrete with nanomaterials embedded PCM for passive cooling application in buildings." *Mater. Today: Proc.* 28 (Jan): 1054–1063. https://doi.org/10.1016/j.matpr.2019.12.356.

Royon, L., L. Karim, and A. Bontemps. 2013. "Thermal energy storage and release of a new component with PCM for integration in floors for thermal management of buildings." *Energy Build.* 63 (Aug): 29–35. https://doi.org/10.1016/j.enbuild.2013.03.042.

Saeed, R. M., J. P. Schlegel, C. Castano, R. Sawafta, and V. Kuturu. 2017. "Preparation and thermal performance of methyl palmitate and lauric acid eutectic mixture as phase change material (PCM)." *J. Storage Mater.* 13 (Oct): 418–424. https://doi.org/10.1016/j.est.2017.08.005.

Saffari, M., A. de Gracia, S. Ushak, and L. F. Cabeza. 2017. "Passive cooling of buildings with phase change materials using whole-building energy simulation tools: A review." *Renewable Sustainable Energy Rev.* 80 (Dec): 1239–1255. https://doi.org/10.1016/j.rser.2017.05.139.

Sarbu, I., and C. Sebarchievici. 2018. "A comprehensive review of thermal energy storage." *Sustainability* 10 (1): 191. https://doi.org/10.3390/su10010191.

Sarı, A. 2004. "Form-stable paraffin/high density polyethylene composites as solid–liquid phase change material for thermal energy storage: Preparation and thermal properties." *Energy Convers. Manage.* 45 (13–14): 2033–2042. https://doi.org/10.1016/j.enconman.2003.10.022.

Sata, V., J. Tangpagasit, C. Jaturapitakkul, and P. Chindaprasirt. 2012. "Effect of W/B ratios on pozzolanic reaction of biomass ashes in Portland cement matrix." *Cem. Concr. Compos.* 34 (1): 94–100. https://doi.org/10.1016/j.cemconcomp.2011.09.003.

Shen, Y., S. Liu, C. Zeng, Y. Zhang, Y. Li, X. Han, and L. Yang. 2021. "Experimental thermal study of a new PCM-concrete thermal storage block (PCM-CTSB)." *Constr. Build. Mater.* 293 (Jul): 123540. https://doi.org/10.1016/j.conbuildmat.2021.123540.

Shi, X., S. A. Memon, W. Tang, H. Cui, and F. Xing. 2014. "Experimental assessment of position of macro encapsulated phase change material in concrete walls on indoor temperatures and humidity levels." *Energy Build.* 71 (Mar): 80–87. https://doi.org/10.1016/j.enbuild.2013.12.001.

Song, H., W. S. Yum, S. Sim, D. Jeon, S. Yoon, and J. E. Oh. 2022. "Proposed specific heat capacity model for a concrete wall containing phase change material (PCM) under field experiment conditions." *Constr. Build. Mater.* 336 (Jun): 127381. https://doi.org/10.1016/j.conbuildmat.2022.127381.

Souayfane, F., F. Fardoun, and P. H. Biwole. 2016. "Phase change materials (PCM) for cooling applications in buildings: A review." *Energy Build.* 129 (Oct): 396–431. https://doi.org/10.1016/j.enbuild.2016.04.006.

Stritih, U., and V. Butala. 2011. "Energy savings in building with a PCM free cooling system." *Strojniški Vestnik* 57 (2): 125–134. https://doi.org/10.5545/sv-jme.2010.066.

Su, W., J. Darkwa, and G. Kokogiannakis. 2015. "Review of solid–liquid phase change materials and their encapsulation technologies." *Renewable Sustainable Energy Rev.* 48 (Aug): 373–391. https://doi.org/10.1016/j.rser.2015.04.044.

Wang, H., W. Lu, Z. Wu, and G. Zhang. 2020. "Parametric analysis of applying PCM wallboards for energy saving in high-rise lightweight buildings in Shanghai." *Renewable Energy* 145 (Jan): 52–64. https://doi.org/10.1016/j.renene.2019.05.124.

Wang, J., J. K. Carson, M. F. North, and D. J. Cleland. 2006. "A new approach to modelling the effective thermal conductivity of heterogeneous materials." *Int. J. Heat Mass Transfer* 49 (17–18): 3075–3083. https://doi.org/10.1016/j.ijheatmasstransfer.2006.02.007.

Wen, R., X. Zhang, Y. Huang, Z. Yin, Z. Huang, M. Fang, and X. Wu. 2017. "Preparation and properties of fatty acid eutectics/expanded perlite and expanded vermiculite shape-stabilized materials for thermal energy storage in buildings." *Energy Build.* 139 (Mar): 197–204. https://doi.org/10.1016/j.enbuild.2017.01.025.

Yeon, J. H. 2020. "Thermal behavior of cement mortar embedded with low-phase transition temperature PCM." *Constr. Build. Mater.* 252 (Aug): 119168. https://doi.org/10.1016/j.conbuildmat.2020.119168.

Zhang, S., D. Feng, L. Shi, L. Wang, Y. Jin, L. Tian, and Y. Yan. 2021. "A review of phase change heat transfer in shape-stabilized phase change materials (SS-PCMs) based on porous supports for thermal energy storage." *Renewable Sustainable Energy Rev.* 135 (Jan): 110127. https://doi.org/10.1016/j.rser.2020.110127.

Zhang, X., M. Xu, L. Liu, C. Huan, Y. Zhao, C. Qi, and K. I. Song. 2020. "Experimental study on thermal and mechanical properties of cemented paste backfill with phase change material." *J. Mater. Res. Technol.* 9 (2): 2164–2175. https://doi.org/10.1016/j.jmrt.2019.12.047.